SANDIA REPORT
SAND2014-17474
Unlimited Release
Printed Month and Year

Investigation of Wave Energy Converter Effects on the Nearshore Environment: A Month-Long Study in Monterey Bay, CA

Grace Chang, Jason Magalen, Craig Jones, and Jesse Roberts

Prepared by
Sandia National Laboratories
Albuquerque, New Mexico 87185 and Livermore, California 94550

Sandia National Laboratories is a multi-program laboratory managed and operated by Sandia Corporation, a wholly owned subsidiary of Lockheed Martin Corporation, for the U.S. Department of Energy's National Nuclear Security Administration under contract DE-AC04-94AL85000.

Issued by Sandia National Laboratories, operated for the United States Department of Energy by Sandia Corporation.

Available to DOE and DOE contractors from
U.S. Department of Energy
Office of Scientific and Technical Information
P.O. Box 62
Oak Ridge, TN 37831

Telephone: (865) 576-8401
Facsimile: (865) 576-5728
E-Mail: reports@adonis.osti.gov
Online ordering: http://www.osti.gov/bridge

Available to the public from
U.S. Department of Commerce
National Technical Information Service
5285 Port Royal Rd.
Springfield, VA 22161

Telephone: (800) 553-6847
Facsimile: (703) 605-6900
E-Mail: orders@ntis.fedworld.gov
Online order: http://www.ntis.gov/help/ordermethods.asp?loc=7-4-0#online

SAND2014-17474
Unlimited Release
Printed Month Year

Investigation of Wave Energy Converter Effects on the Nearshore Environment: A Month-Long Study in Monterey Bay, CA

Grace Chang, Jason Magalen, and Craig Jones
Sea Engineering, Inc.
200 Washington Street, Suite 101
Santa Cruz, CA 95060

Jesse Roberts
Water Power
Sandia National Laboratories
P.O. Box 5800
Albuquerque, New Mexico 87185-MS1124

Abstract

A modified version of an industry standard wave modeling tool, SNL-SWAN, was used to perform model simulations for hourly initial wave conditions measured during the month of October 2009. The model was run with an array of 50 wave energy converters (WECs) and compared with model runs without WECs. Maximum changes in H_s were found in the lee of the WEC array along the angles of incident wave direction and minimal changes were found along the western side of the model domain due to wave shadowing by land. The largest wave height reductions occurred during observed typhoon conditions and resulted in 14% decreases in H_s along the Santa Cruz shoreline. Shoreline reductions in H_s were 5% during south swell wave conditions and negligible during average monthly wave conditions.

ACKNOWLEDGMENTS

The research and development described in this document was funded by the U.S. Department of Energy. Sandia is a multiprogram laboratory operated by Sandia Corporation, a Lockheed Martin Company, for the United States Department of Energy's National Nuclear Security Administration under contract DE-AC04-94AL85000.

This research was made possible by support from the Department of Energy's Wind and Water Power Technologies Office.

CONTENTS

FIGURES

TABLES

NOMENCLATURE

CCW	Counter clockwise
CW	Clockwise
DOE	Department of Energy
F-2HB	Floating two-body heaving converter
F-OWC	Floating oscillating water column
H_s	Significant wave height
Kt	Transmission coefficient
Ktp	1 – RCW
kW	Kilowatt
mdc	Directional resolution
MWD	Mean wave direction
NDBC	National Data Buoy Center
NOAA	National Oceanic and Atmospheric Administration
PTO	Power take-off
RCW	Relative capture width
SNL	Sandia National Laboratories
SWAN	Simulating WAves Nearshore
SNL-SWAN	Modified SWAN model
T_p	Peak wave period
WEC	Wave energy converter

1. INTRODUCTION

To effectively generate commercial-scale power for an electric grid, wave energy converters (WECs) need to be installed in arrays comprising multiple devices to efficiently convert wave energy into electrical power onshore. The deployment of WEC arrays will begin small (pilot-scale or ~10 devices) but could feasibly number in the hundreds of individual devices at commercial-scale. As the industry progresses from pilot- to commercial-scale, it is important to understand and quantify the relationship between the number of installed devices and the device-specific characteristics with the potential to affect the natural nearshore processes that support a local, healthy ecosystem.

Of consideration here is the potential for WEC arrays to alter nearshore wave propagation and circulation patterns, possibly modifying sediment transport patterns and ecosystem processes. As WEC array sizes grow, there is a potential for negative environmental impacts which could be detrimental to local coastal ecology, and social and economic services. To help accelerate the realization of commercial-scale wave power, predictive modeling tools are developed and utilized to investigate ranges of anticipated scenarios and evaluate the potential for both positive and negative environmental impact.

The present study incorporated a modified version of an industry standard wave modeling tool, SWAN (Simulating WAves Nearshore), to simulate wave propagation through a hypothetical WEC array deployment site on the California coast. The modified SWAN model, SNL-SWAN, was conducted in hindcast mode using recorded wave parameter boundary conditions. The primary objective of the present study was to investigate the effects of a WEC array on nearshore wave propagation, given actual wave conditions. To accomplish this, the following tasks were undertaken:

(1) Obtain model boundary conditions: hourly time series of offshore wave parameters measured in Monterey Bay, CA in October 2009 when known variability in wave height, period, and direction was observed.
(2) Perform SNL-SWAN wave propagation simulations for two different types of WEC device types using the Monterey Bay, CA offshore wave parameter data.
(3) Investigate the modeled nearshore wave conditions in the presence and absence of WEC array(s).

2. OFFSHORE WAVE PARAMETERS

Hourly wave conditions measured in Monterey Bay, CA were obtained from the National Oceanic and Atmospheric Administration's (NOAA's) National Data Buoy Center (NDBC) (http://www.ndbc.noaa.gov/). Data were from NDBC Station 46042, located 27 nautical miles west-northwest of Monterey, CA (36.785°N, 122.469°W) in 2098 m water depth. Data have been recorded at this location since 1987, making it a statistically reliable source for evaluating typical and extreme wave conditions approaching Monterey Bay.

Frequency distributions of significant wave height, peak wave period, and mean wave direction for data recorded between 1992 and 2009 by NDBC Station 46042 are shown in Figure 1, Figure 2, and Figure 3. Significant wave height is the average of the highest 1/3 of wave heights on record. Peak wave periods correspond directly to the frequency containing the largest amount of wave energy. Mean wave directions are the directions *from* which the dominant waves (waves corresponding to the dominant period) are approaching.

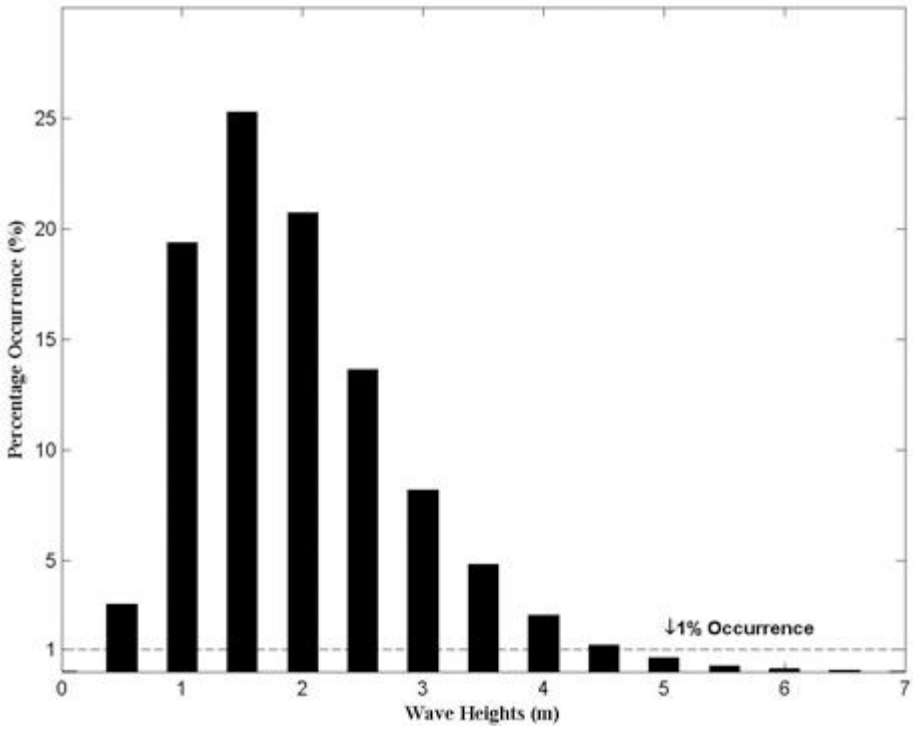

Figure 1. Significant wave height frequency of occurrence distribution (histogram) for data collected between 1992 and 2009 by NOAA NDBC Station 46042.

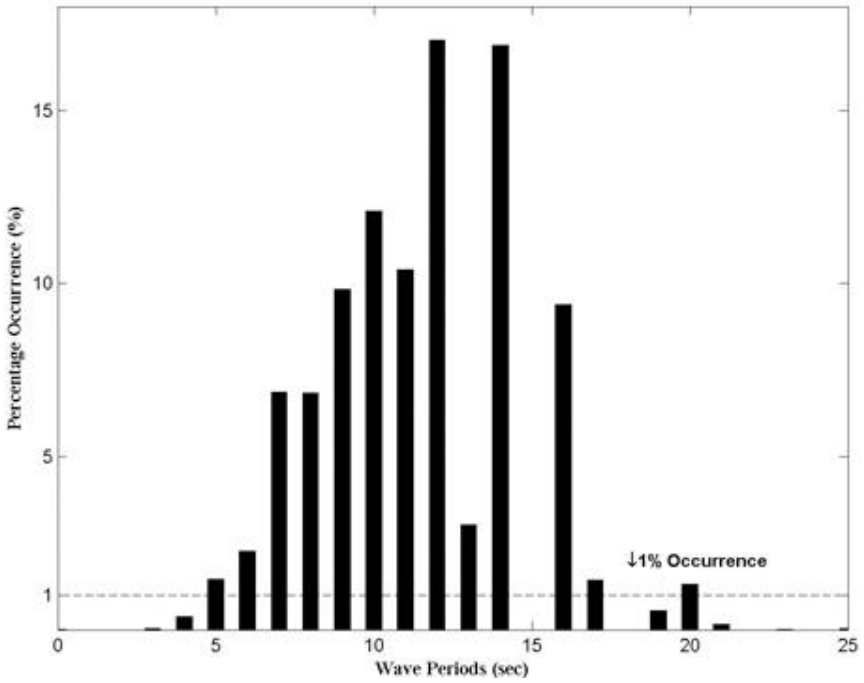

Figure 2. Peak wave period frequency of occurrence distribution (histogram) for NOAA NDBC Station 46042 data collected between 1992 and 2009.

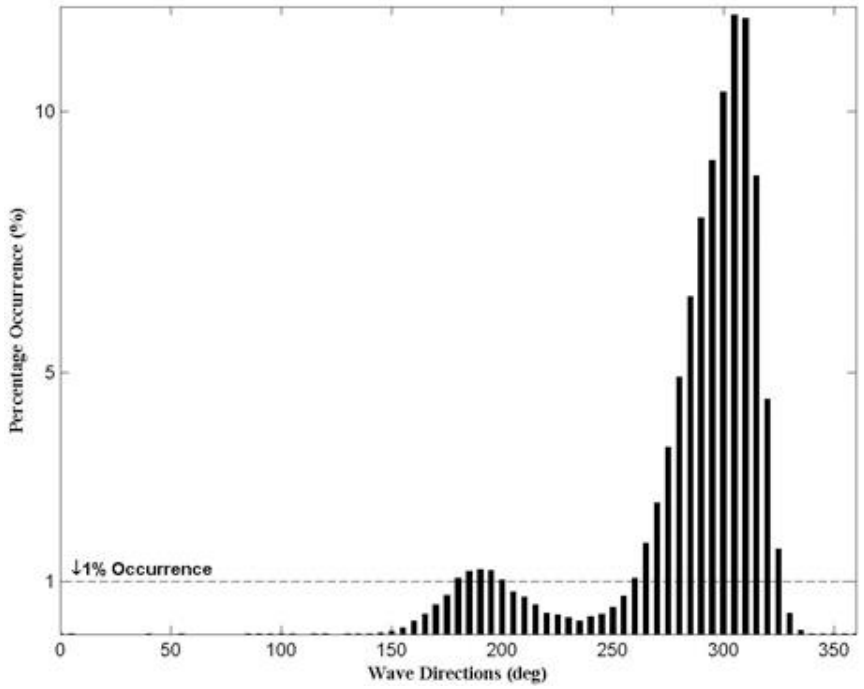

Figure 3. Mean wave direction frequency of occurrence distribution (histogram) for NOAA NDBC Station 46042 data collected between 1992 and 2009.

The period between 1 and 31 October 2009 was chosen for wave, hydrodynamic, and sediment transport simulations because a variety of wave conditions were observed in Monterey Bay, CA during that time, including a storm that was the remnant of a western Pacific typhoon and several south swells. Significant wave heights ranged between 0.9 and 5.63 meters, peak wave periods ranged between 4.55 and 19.05 seconds, and mean wave direction varied between 161 and 334 degrees in October 2009 (Table 1 and Figure 4). The wave conditions observed during the typhoon that passed Monterey Bay, CA on 13 and 14 October 2009 (H_s = 5 m; MWD = 161°) occurred less than 1% of the time in the 18 year period between 1992 and 2009.

Table 1. Wave parameter statistics for data collected by NOAA NDBC buoy 46042 in October 2009.

Parameter*	Mean	Min	Max	STD
H_s (m)	2.34	0.90	5.63	0.99
T_p (s)	11.15	4.55	19.05	2.76
MWD (deg)	288.03	161.00	334.00	41.59

*H_s = significant wave height; T_p = peak period; MWD = mean wave direction.

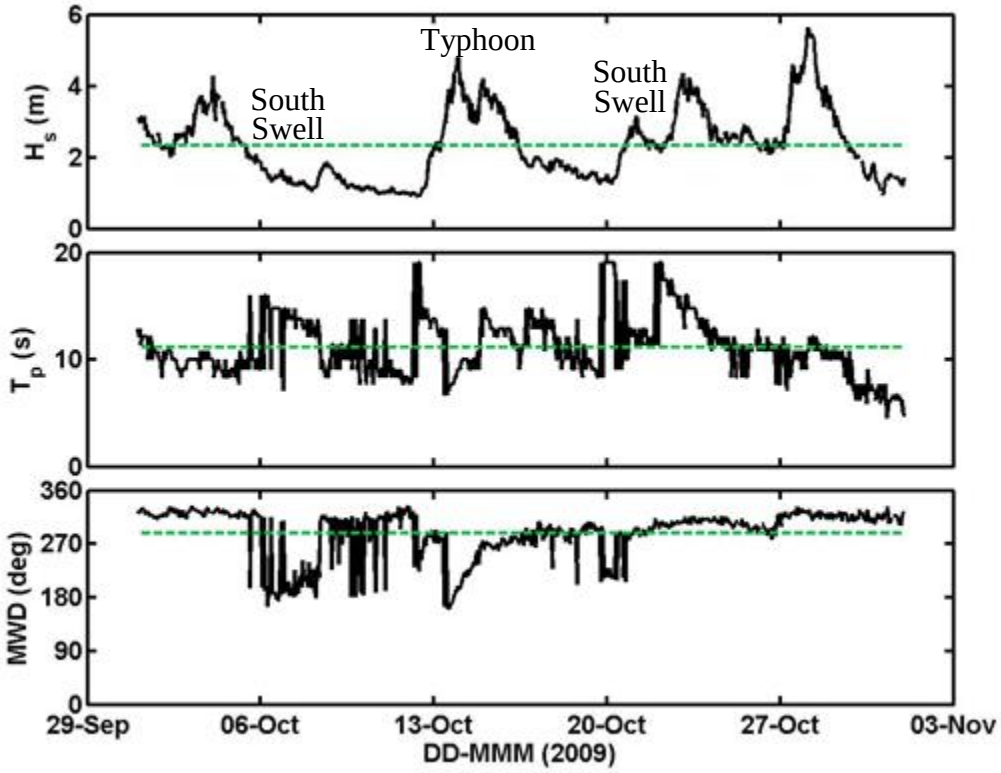

Figure 4. Time series of significant wave height (H_s), peak period (T_p), and mean wave direction (MWD) recorded by NDBC Station 46042 in October 2009. Mean values are indicated by dashed green lines. Significant events are labeled.

3. SNL-SWAN WAVE PROPAGATION SIMULATIONS

The October 2009 Monterey Bay, CA offshore wave parameter data obtained from NOAA NDBC were propagated from offshore to onshore using SNL-SWAN. The wave propagation simulations were performed for two different types of WEC device types, modeled as obstacles in SNL-SWAN. Results were evaluated at specific nearshore coastal locations, as described below in further detail.

3.1. Model Domain

Similar to previous SWAN WEC device modeling efforts, the selected modeling site was near-shore Monterey Bay and Santa Cruz, California. Two SNL-SWAN model grids were nested to predict the propagation of deep-water waves from offshore of Monterey Bay, CA, to nearshore Santa Cruz, CA. The Monterey Bay and Santa Cruz model domains are shown in Figure 5 and Figure 6. The coarse-grid (herein referred to as the Monterey Bay model domain) resolution was approximately 0.001° degrees in latitude and longitude (approximately 100 m grid spacing in x and y). SNL-SWAN was run as a stationary model; hydrodynamic conditions at the offshore boundaries were kept constant. Directional wave energy spectra conditions were exported from the coarse resolution model and used as boundary conditions for the nested, fine resolution model (herein referred to as the Santa Cruz model domain).

The grid resolution of the nested Santa Cruz model domain computational grid was matched to the size of the modeled WEC device type, or SWAN obstacle. For model runs, the device types chosen were the 20-m floating two-body heaving converter (F-2HB) and the 50 m floating oscillating water column buoy (F-OWC; Babarit, 2012). These devices, because of their relatively large size, were found to have the most significant effects on nearshore wave propagation (Chang et al., 2014). The Santa Cruz model grid size was therefore approximately 0.00020° or 0.00050° in latitude and longitude for model runs with the F-2HB or F-OWC device type, respectively. The wave spectrum boundary conditions were applied along the offshore boundaries of the Santa Cruz SNL-SWAN model domain. The nested grid model was also implemented as a stationary model.

The offshore model boundary conditions were specified for all “wet” boundaries (north, west and south sides) of the Monterey Bay domain. Hourly wave conditions (H_s, T_p, and MWD) obtained from NDBC station 46042 during the period of 1 – 31 October 2009 were propagated from offshore to onshore throughout the entire domain. Wave frequency and directional spectra were extracted along the “wet” boundaries of the Santa Cruz domain and used as input boundary conditions for the nested Santa Cruz domain (Figure 5 and Figure 6). Waves were then propagated from the offshore boundaries of the Santa Cruz model domain to the shoreline and evaluated at specified nearshore locations.

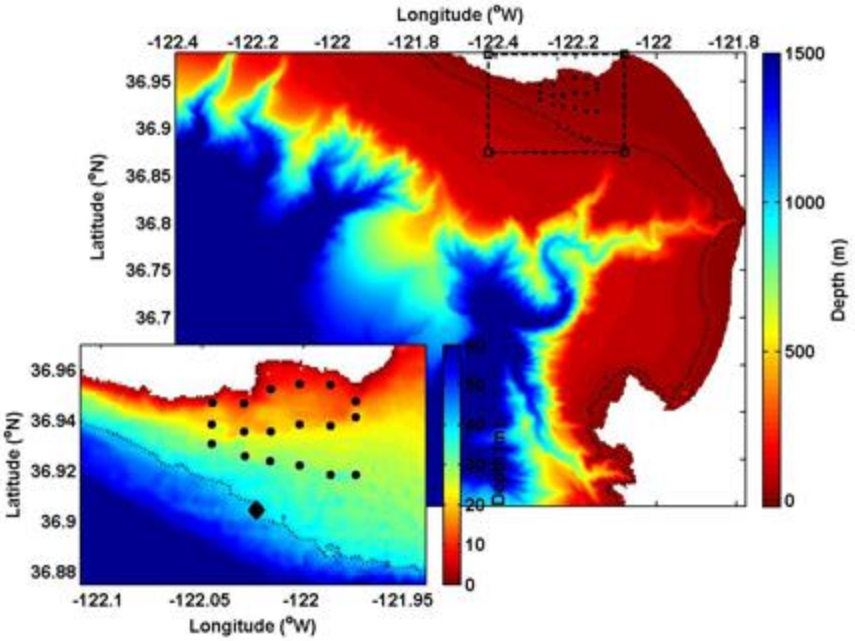

Figure 5. Monterey Bay and Santa Cruz model domains (40 m depth contour indicated). The inset shows the Santa Cruz domain. The diamond centered on the 40 m contour in the Santa Cruz domain indicates the simulated WEC array comprising of 50 F-2HB device types. The black dots shown in both model domains are the model evaluation locations.

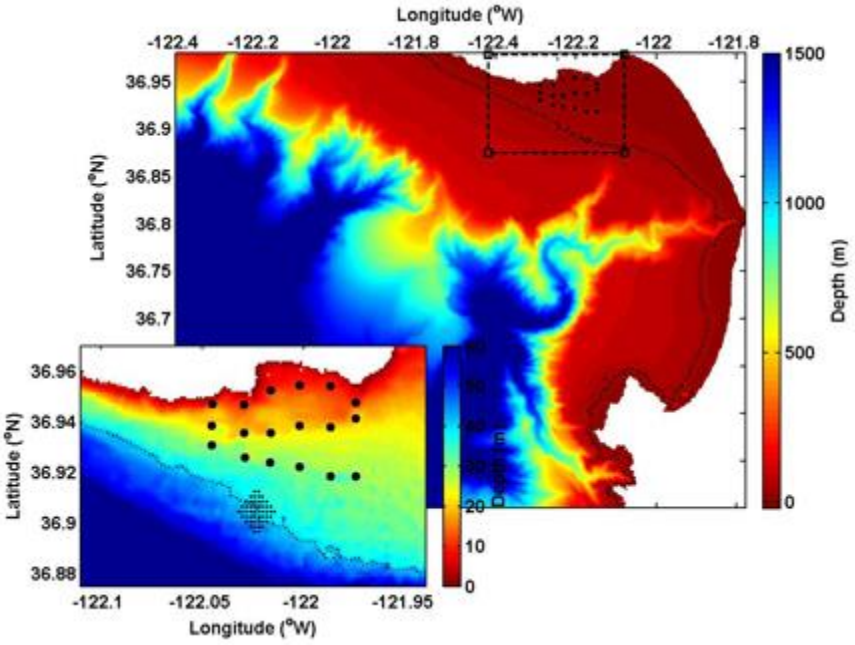

Figure 6. Same caption as in Figure 5 but for 50 F-OWC device types.

3.2 Simulated WEC Devices

The modified SWAN wave model, SNL-SWAN, attempts to incorporate device-specific WEC power take-off (PTO) characteristics to more accurately evaluate each device's effects on wave propagation and ultimately nearshore hydrodynamics. SNL-SWAN calculates the relative capture width (RCW) or ratio of incident wave power to captured wave power by a specific WEC device given the initial wave conditions (e.g., H_s, T_p, and MWD). The RCW value is then returned to the SWAN program and is used for calculation of the wave energy transmission coefficient, Kt, for the WEC device. The device is specified as an obstacle to propagating wave energy in SWAN, where:

$$Kt = \text{sqrt}(Ktp) \text{ and}$$
$$Ktp = 1 - RCW.$$

Three methods of determining the transmission coefficient are employed in SNL-SWAN, corresponding to the operator-set value of the switch in the model. Hereafter, these are referred to as "switch 0", "switch 1" and "switch 2", respectively, where:

Switch 0) SNL-SWAN defers to the native SWAN code, i.e. the transmission coefficient is user-specified in the INPUT file,

Switch 1) SNL-SWAN computes the RCW from a user-supplied device-specific power matrix, or

Switch 2) User-supplied RCW for a specific wave height and period.

In the present analysis, Switch 1 was utilized for WEC device arrays comprising of 50 buoys arranged in a honeycomb/diamond-shape as a representative configuration (Figure 7). WEC devices were simulated with 4-diameter spacing between devices, center to center. Devices were equally spaced in all directions (Figure 7). As mentioned in Section 3.1, the two modeled devices were the floating two-body heaving converter (F-2HB) and floating oscillating water column (F-OWC) WECs, which are 20 m and 50 m in diameter, respectively.

The power matrices for the F-2HB and F-OWC devices are shown in Figure 8. These power matrices were computed based on the numerical approach described by Babarit et al. (2012). Both WEC device types are optimized in terms of its power at significant wave heights of greater than 4 m and peak wave periods between 8 and 12 s. However, the F-OWC WEC captures about twice the amount of power (2000 kW) as the F-2HB device (1000 kW) in this range of optimal wave conditions.

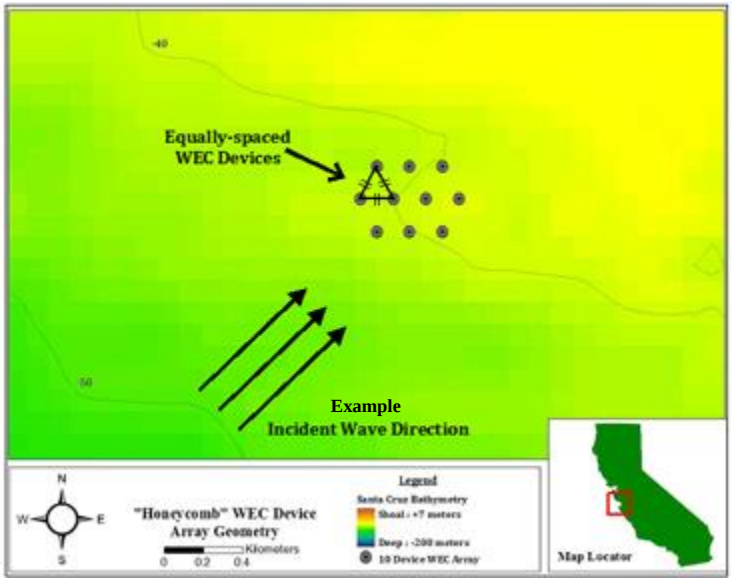

Figure 7. Example honeycomb geometry of a WEC device array in the model. Here, 10 WECs are illustrated with an example incident mean wave direction of 205°.

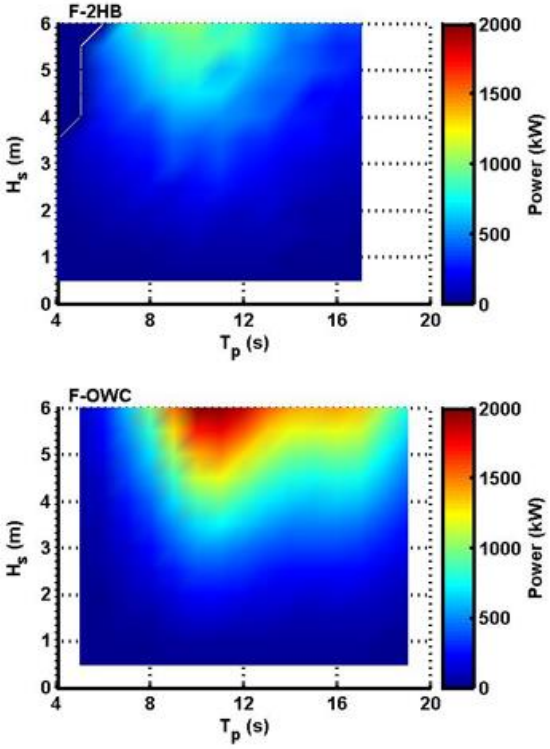

Figure 8. Power matrices computed for the F-2HB WEC device (upper panel) and the F-OWC WEC device (lower panel) as a function of significant wave height and peak wave period.

3.3. Model Output Locations

In order to evaluate the effects of the WEC array on wave propagation for a variety of wave conditions, model output was extracted at 18 distinct locations (Table 2 and **Error! Reference source not found.**). Six shoreline locations along the Santa Cruz coast were selected to span the anticipated horizontal extent of wave shadowing due to the WEC arrays (West to East):

- West Santa Cruz
- Steamer Lane
- Santa Cruz Wharf
- Santa Cruz Harbor
- East 26th Ave.
- Pleasure Point

Model output extraction occurred at three depth contours offshore of each shoreline location: the 30 m, 20m and 10 m depth contours, oriented and numbered sequentially south to north and west to east (see numbering in Table 2 and Figure 9).

These regions of the Santa Cruz shoreline are popular sight-seeing, surfing and recreation locations, with surf breaks, jogging paths and residential homes extending along the headlands and the beaches. Changes in nearshore wave conditions due to the WEC array, if any, are important to ascertain at this location since this will likely concern the recreational community. Furthermore, changes in wave conditions at these nearshore locations are important to evaluate from the perspective of tidal circulation, shoreline erosion, and ecological change.

Table 2. Model output location number, depth contour, and descriptions.

Model Output Location	Depth Contour and Description
1	30 m - West Santa Cruz
2	30 m - Steamer Lane
3	30 m – Santa Cruz Wharf
4	30 m – Santa Cruz Harbor
5	30 m – East 26th Ave
6	30 m - Pleasure Point
7	20 m - West Santa Cruz
8	20 m - Steamer Lane
9	20 m – Santa Cruz Wharf

Model Output Location	Depth Contour and Description
10	20 m – Santa Cruz Harbor
11	20 m – East 26th Ave
12	20 m - Pleasure Point
13	10 m - West Santa Cruz
14	10 m - Steamer Lane
15	10 m – Santa Cruz Wharf
16	10 m – Santa Cruz Harbor
17	10 m – East 26th Ave
18	10 m - Pleasure Point

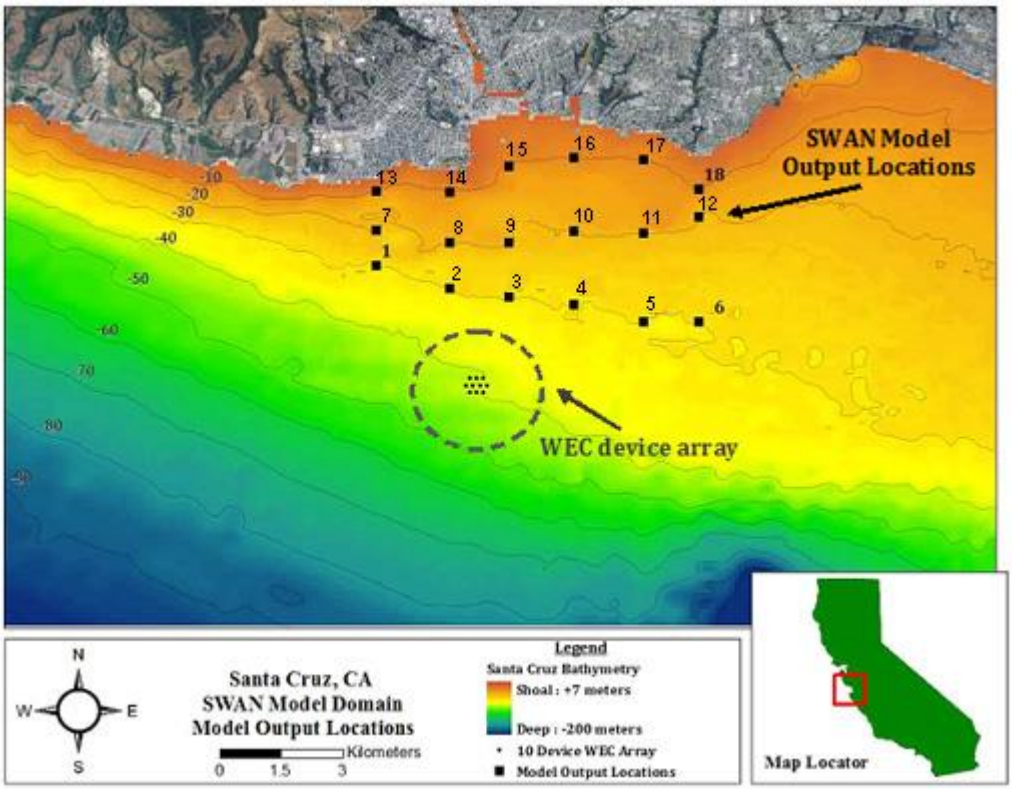

Figure 9. Santa Cruz domain with example WEC device array (gray dashed circle) and model output locations (black squares) shown.

4. SNL-SWAN MODEL RESULTS

Model runs were conducted for hourly NDBC data available between October 1 and October 31, 2009, for a total of 2,972 model runs (743 hours each for F-2HB and F-OWC in addition to 743 hours each for model runs with no obstacles with 20 m and 50 m grid spacing). Model results with simulated WECs were compared to model runs conducted with no obstacles. All model runs were conducted with 9° directional resolution (mdc = 40), zero wave energy reflection allowed, no diffraction, and the WEC array centered on the 40 m depth contour, as shown in Figure 7.

The initial wave conditions were obtained from NOAA NDBC station 46042 and shown in Figure 4. Note that no wave parameter data were available from NOAA NDBC for 14 data points over the 31 day period in October 2009. These data points were specified as "NaN" (not-a-number) and not included in any subsequent analyses.

Model results were retained for each model run. Results included propagated wave heights, wave periods, and wave directions at all grid points in the Santa Cruz model domain. Further, the same wave properties were extracted at each of the 18 distinct model output locations to facilitate point-to-point comparison.

The time series results for both WEC types are shown in **Error! Reference source not found.** through **Error! Reference source not found.**. The results are comparisons for both WEC types, comparing the modeled scenario results to the baseline scenario results, where the baseline scenario does not include WEC devices. Each figure shows results at six of the 18 output points, located on same depth contour: 10 m, 20 m, or 30 m. Significant wave height and peak wave period results are presented in percentage change from the baseline scenario, computed as:

$$Percentage\ Change = \frac{(InitialValue - FinalValue)}{InitialValue} \times 100. \qquad \text{Eq. 1}$$

Therefore, a positive change indicates a decrease in the value of the wave parameter in the presence of a WEC array and *vice versa*. Mean wave direction results are presented as the difference between the modeled scenario and the baseline scenario, or:

$$Difference = InitialValue - FinalValue. \qquad \text{Eq. 2}$$

Negative changes in mean wave direction indicate clockwise (CW) rotation of wave direction. Positive changes indicate counter-clockwise (CCW) rotation.

4.1 Significant Wave Height

Results of significant wave height predictions from the model runs with 50 F-2HB or F-OWC WECs are shown in Figure 10, Figure 11, and Figure 12. Significant wave shadowing by land to the west of the study site was found for mean wave directions from the northwest (>270°). Wave height reduction of greater than 0.5% was found only during periods of swell angle less than about 270° except for output locations 5 and 6. These output locations, located to the east of the study site on the 30 m depth contour, exhibited small (~1%) wave height decreases during most

wave conditions observed in October 2009 due to its relative positions. With wave refraction, these output points are in the lee of the WEC array for northwest wave directions.

For the more southerly waves, wave height decreases of nearly 15% were observed for output locations between the WEC array and the shoreline, with generally greater reduction for the offshore output locations (output numbers 1 through 6 in Figure 10). An exception was during the typhoon conditions on 13 and 14 October, when wave focusing was observed, resulting in greater wave reduction at the 10 m depth contour location (output number 14) as compared to output locations along the 20 m or 30 m depth contours (Figure 12). Wave height reduction comparisons for mean conditions (northwest wave direction), initial wave direction from the south, and the typhoon are discussed below.

Wave heights were generally slightly more reduced in the lee of 50 F-OWC WEC device types in comparison to the F-2HB WECs due to the greater power capture capability of the F-OWC WEC (Figure 8). Previous model sensitivity studies revealed that the magnitude of wave height reduction is directly correlated to a WEC's power matrix values, with larger values resulting in more reduction in wave height and *vice versa* (Chang et al., 2014). The temporal variability of wave height reduction was similar between the two device types.

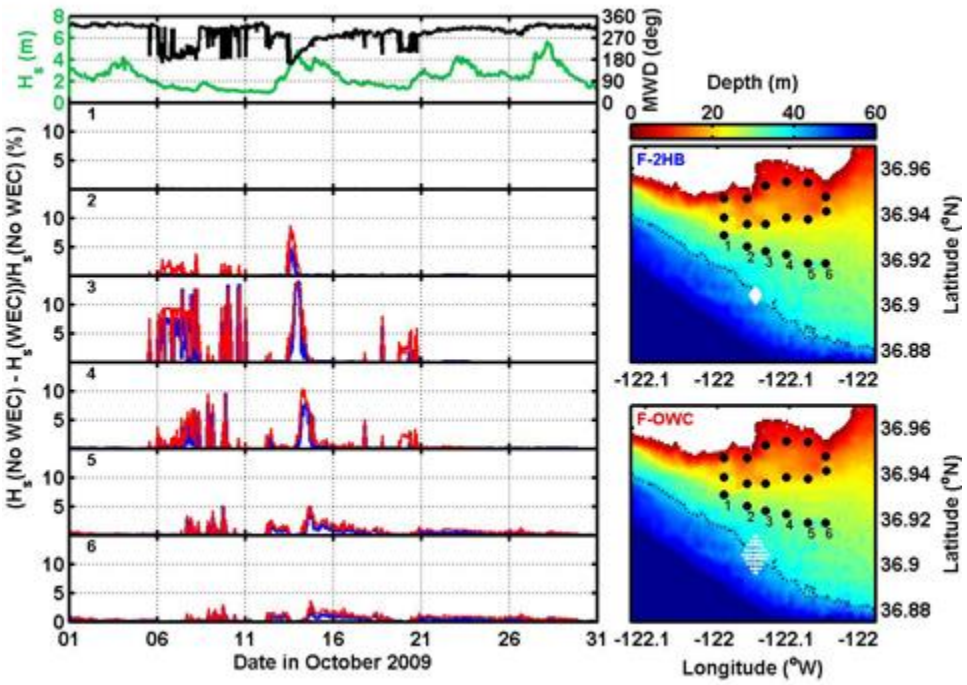

Figure 10. Left: Time series of model input H_s and MWD followed below by comparisons between modeled H_s with WECs and without WECs along the 30 m depth contour. Blue and red lines are comparison results for F-2HB and F-OWC WECs, respectively. Right: Santa Cruz model domain illustrating the locations of the WEC array and output points. Relevant output points are labeled in the left and right panels.

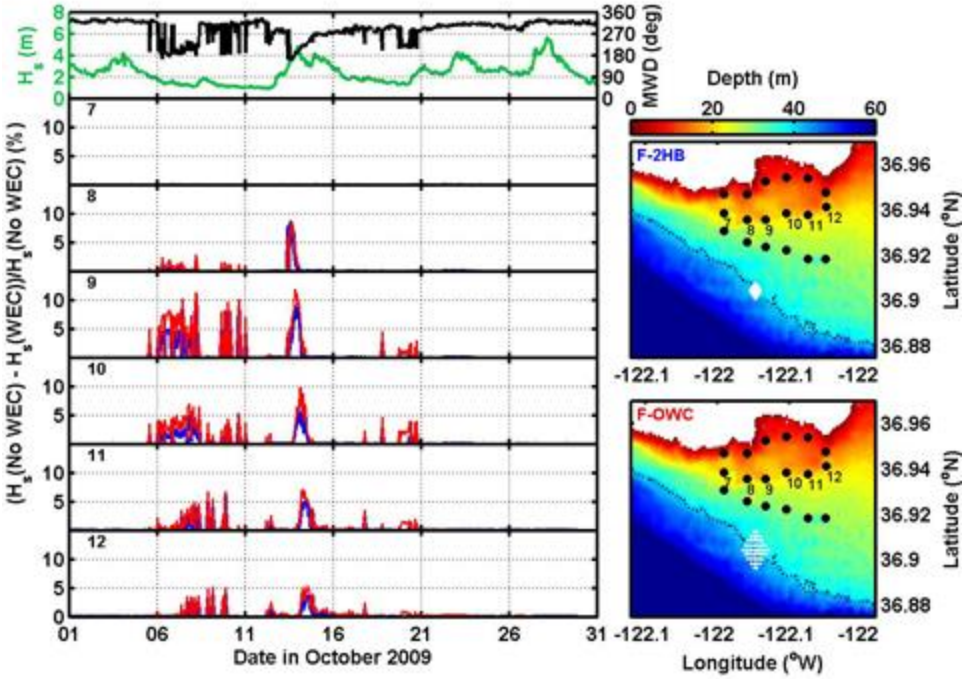

Figure 11. Same as Figure 10 but for model results at output locations along the 20 m depth contour.

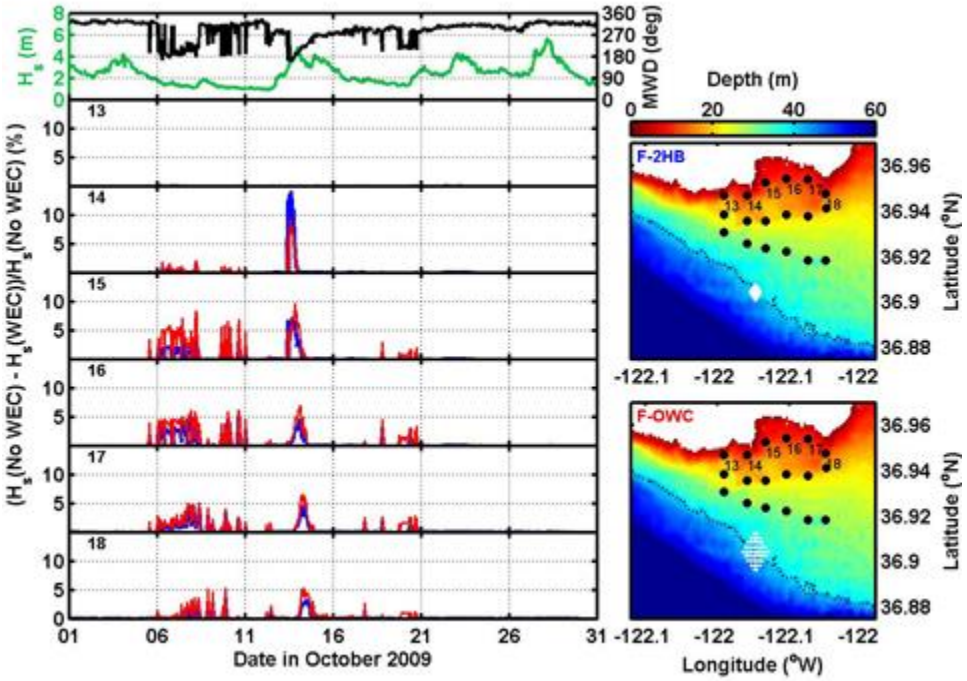

Figure 12. Same as Figure 10 and Figure 11 but for model results at output locations along the 10 m depth contour.

4.2 Peak Wave Periods

The percentage changes in peak wave periods during this study were negligible, as shown in Figure 13, Figure 14, and Figure 15. The reason for this is twofold. First, within the model parameters, the frequency bin resolution may have been too large to register small changes in wave periods (small changes in frequency would not cause a change in frequency bin in model space). Second, since the model obstacles were "absorbing" the same percentage of wave energy from all wave frequencies (i.e. because the transmission coefficient is frequency-independent), there would be no change in peak wave energy; the dominant wave energy would not shift to an alternate frequency(ies). Therefore, in the present study, no change (or negligible change) was observed for all model cases.

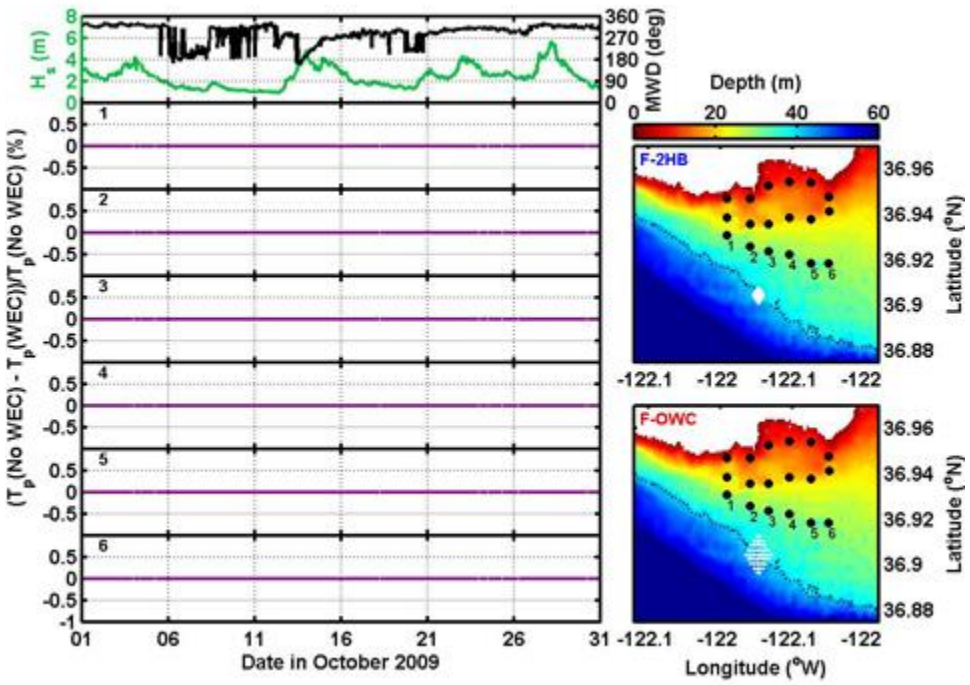

Figure 13. Left: Time series of model input H_s and MWD followed below by comparisons between modeled T_p with WECs and without WECs along the 30 m depth contour. Blue and red lines are comparison results for F-2HB and F-OWC WECs, respectively. Right panels: Santa Cruz model domain illustrating the locations of the WEC array and output points. Relevant output points are labeled in the left and right panels.

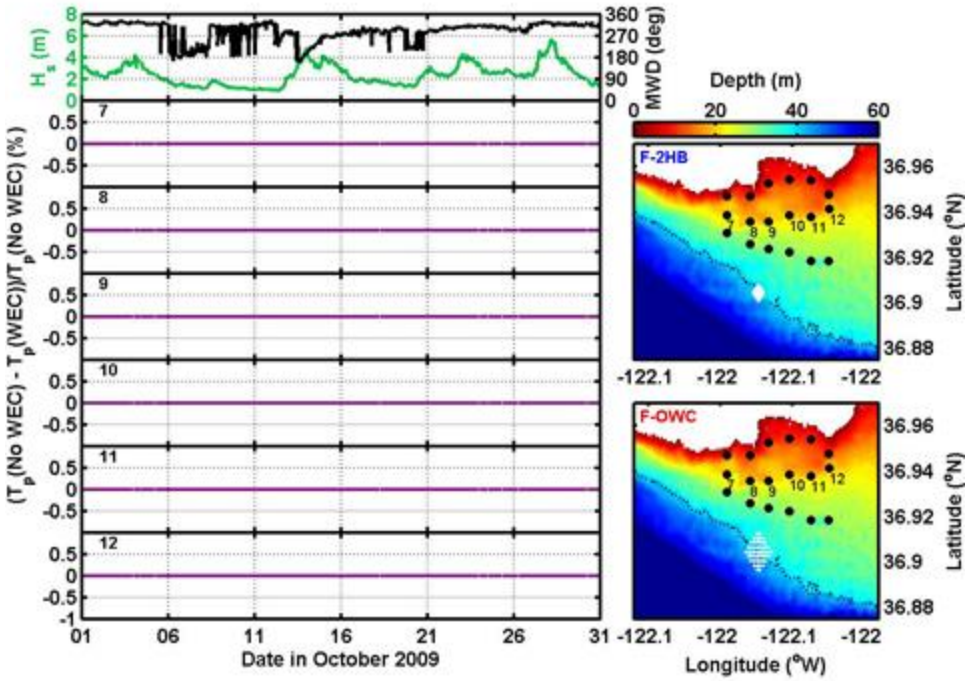

Figure 14. Same as Figure 13 but for model results at output locations along the 20 m depth contour.

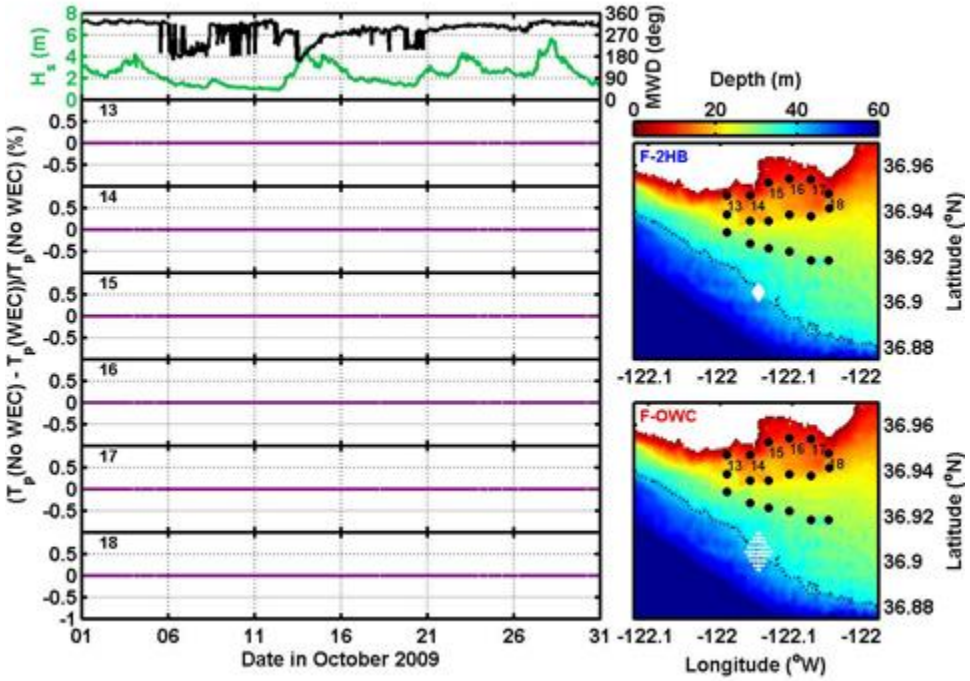

Figure 15. Same as Figure 13 and Figure 14 but for model results at output locations along the 10 m depth contour.

4.3 Mean Wave Directions

Changes in mean wave directions are illustrated in Figure 16, Figure 17, and Figure 18. Recall that negative changes indicated clockwise (CW) rotation of wave direction and positive changes indicated counter-clockwise (CCW) rotation. Rotation, when it occurred in the model, was 9° because the directional bin spacing was equal to 9°. Any changes less than this were indeterminable by the model. It is thus surmised that direction changes, if any, caused by the WEC devices were less than 9°.

Direction changes were not observed at any locations along the western portion of the Santa Cruz model domain (output numbers 1, 7, or 13). Directional changes of ±9° were observed primarily during southerly mean wave directions. During periods when initial wave directions were from the northwest (>270°), direction changes were observed only for eastern output locations (numbers 5, 6, 11, 12, and 18) and more frequently for the F-OWC device type (Figure 16, Figure 17, and Figure 18). The frequency of occurrence of direction change decreased from offshore to onshore (30 m to 10 m depth contour).

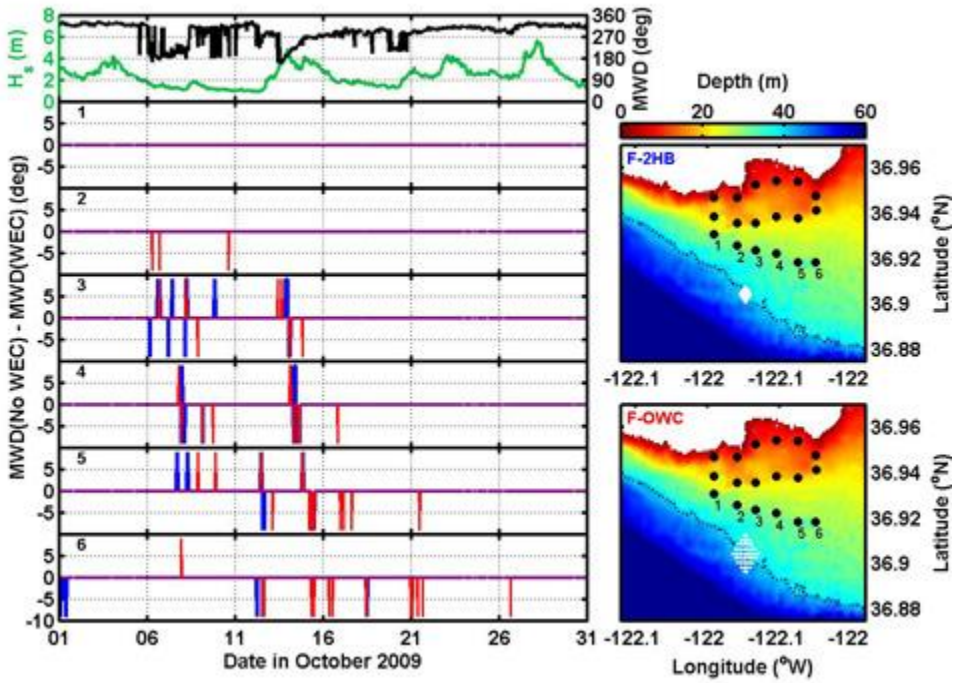

Figure 16. Left: Time series of model input H_s and MWD followed below by comparisons between modeled MWD with WECs and without WECs along the 30 m depth contour. Blue and red lines are comparison results for F-2HB and F-OWC WECs, respectively. Right: Santa Cruz model domain illustrating the locations of the WEC array and output points. Relevant output points are labeled in the left and right panels.

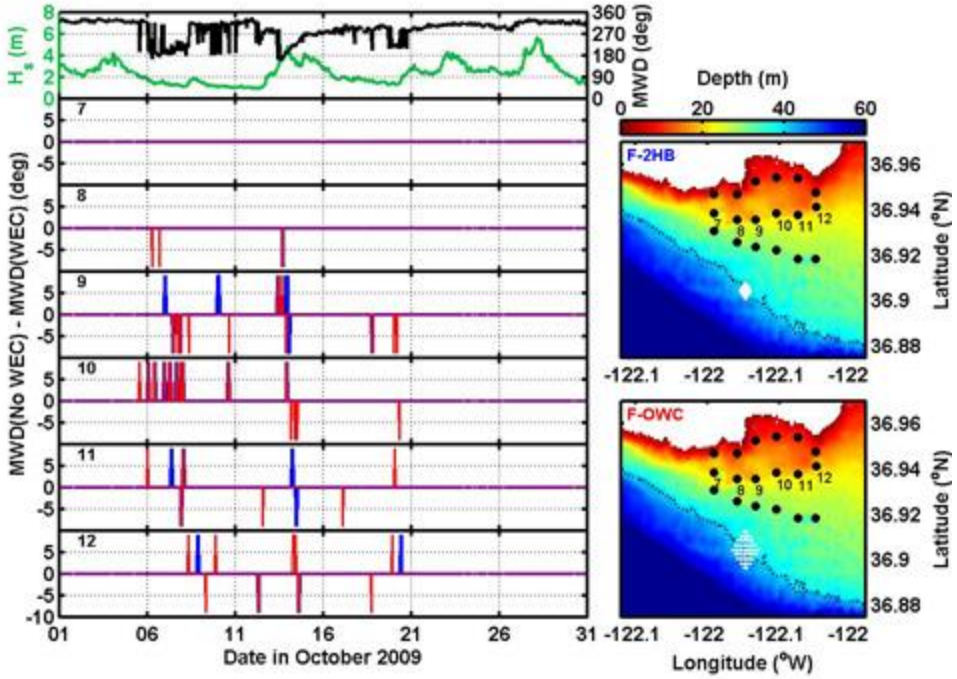

Figure 17. Same as Figure 16 but for model results at output locations along the 20 m depth contour.

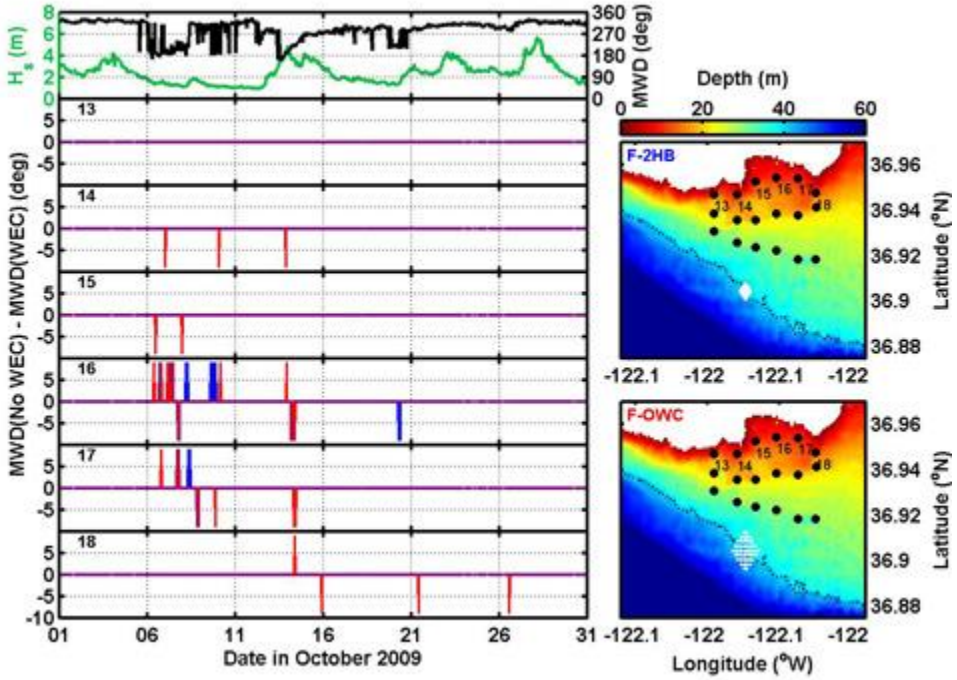

Figure 18. Same as Figure 16 and Figure 17 but for model results at output locations along the 10 m depth contour.

4.4 Northwesterly and Southerly Wave Directions

Comparisons are presented for three initial wave conditions, defined as (date and time of occurrence in parentheses):

1) Average: H_s = 1.77 m, T_p = 12.9 s, and MWD = 288° (17 October 2009, 19:50),
2) South Swell: H_s = 1.15 m, T_p = 12.12 s, and MWD = 180° (8 October 2009, 04:50), and
3) Typhoon: H_s = 3.54 m, T_p = 7.69 s, and MWD = 161° (13 October 2009; 13:50).

Surface-to-surface comparisons are presented to best illustrate the results (Figure 20 through Figure 25). Black coloring in the surface-to-surface comparisons indicates no change in H_s or MWD from the baseline scenario, where baseline is defined as model runs with no WECs. Color bars are included in each figure to indicate the percentage change in H_s or magnitude of change in MWD. Percentage change in H_s from the baseline scenario is computed as described previously in Eq. 1. Surface-to-surface comparisons of mean wave direction are presented as the difference between MWD for model runs with WECs and without WECS (Eq. 2). In addition, the changes computed at each of the 18 model output locations are listed as text in each sub-figure, adjacent to the output location number; this allows for rapid comparisons from case to case. Model run results for the 20 m diameter F-2HB device type are shown for all three wave cases. Results are similar for the 50 m diameter F-OWC device and are not shown here. The frequency of occurrence histograms for H_s, T_p, and MWD during October 2009 are shown in Figure 19.

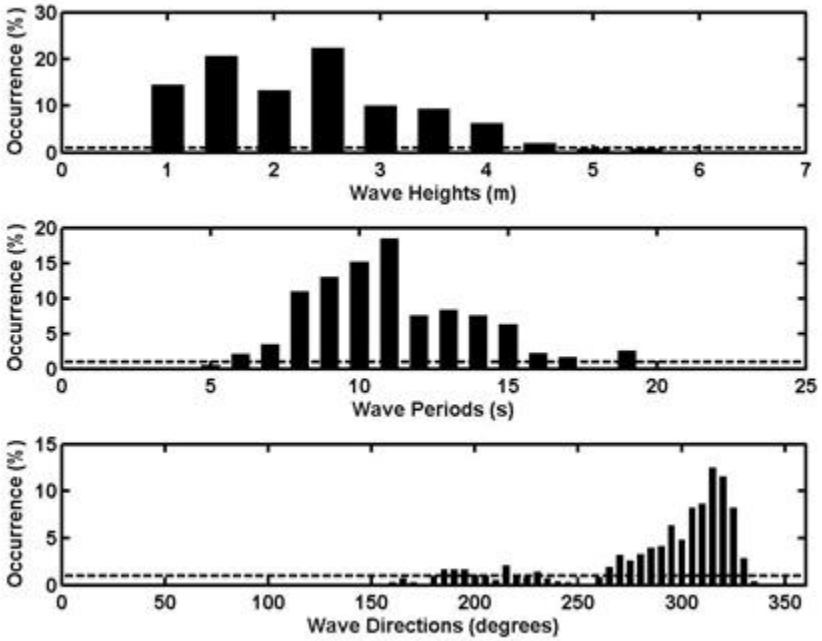

Figure 19. Frequency of occurrence histograms for wave height, period, and direction for NOAA NDBC data collected in October 2009. The dashed lines indicate the 1% occurrence limit.

4.4.1 Average Initial Wave Conditions

As observed in the time series comparisons (Figure 10, Figure 11, and Figure 12), negligible (<0.2%) changes in significant wave height were observed for all output locations except for the easternmost output points on the 30 m depth contour (numbers 5 and 6), which are in the lee of the WEC array for refracted waves originating from the northwest (Figure 20). The percent difference in significant wave height between model runs with and without WECs was small (~1%) at these two locations.

Mean wave directions were not impacted by the WEC array at any of the output locations. However, as shown in Figure 21, negative (clockwise) changes in mean wave direction were observed near the eastern portion of the Santa Cruz model domain. Again, the magnitude of the change was ±9° due to the directional resolution set for the model runs. Any changes less than this were indeterminable by the model.

It can be concluded that during average wave conditions observed in October 2009, a WEC array consisting of 50 F-2HB or F-OWC devices spaced 4-diameters apart had little effect on wave height or direction at the 18 output locations chosen for this modeling study. However, as can be surmised from Figure 20, locations to the east of the Santa Cruz model domain could have been impacted by WECs during average wave conditions for October 2009.

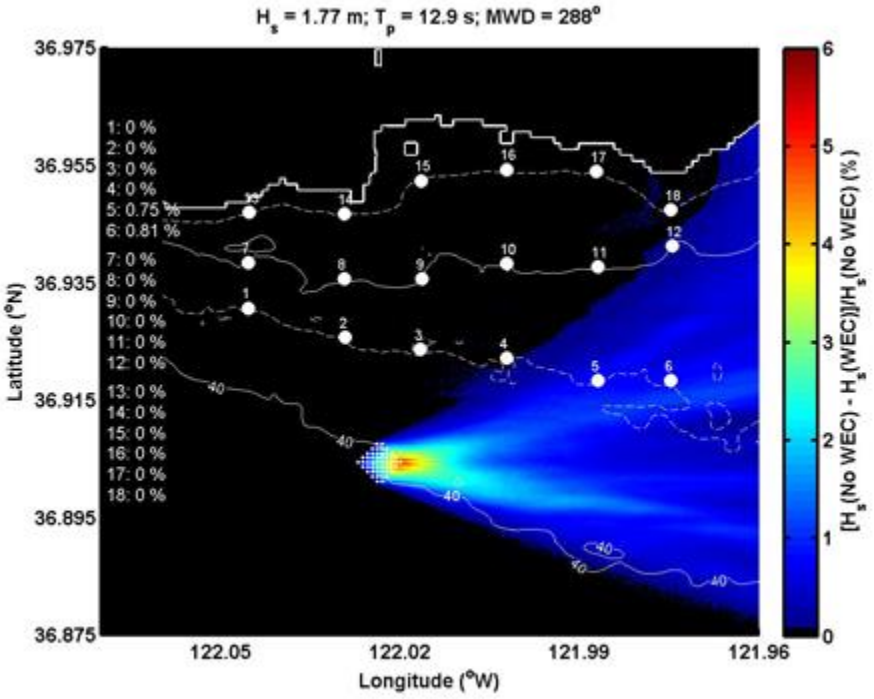

Figure 20. Significant wave height percentage decrease from the baseline scenario for average initial wave conditions. Percent differences at each of the 18 output locations are indicated. Device diameters are not to scale.

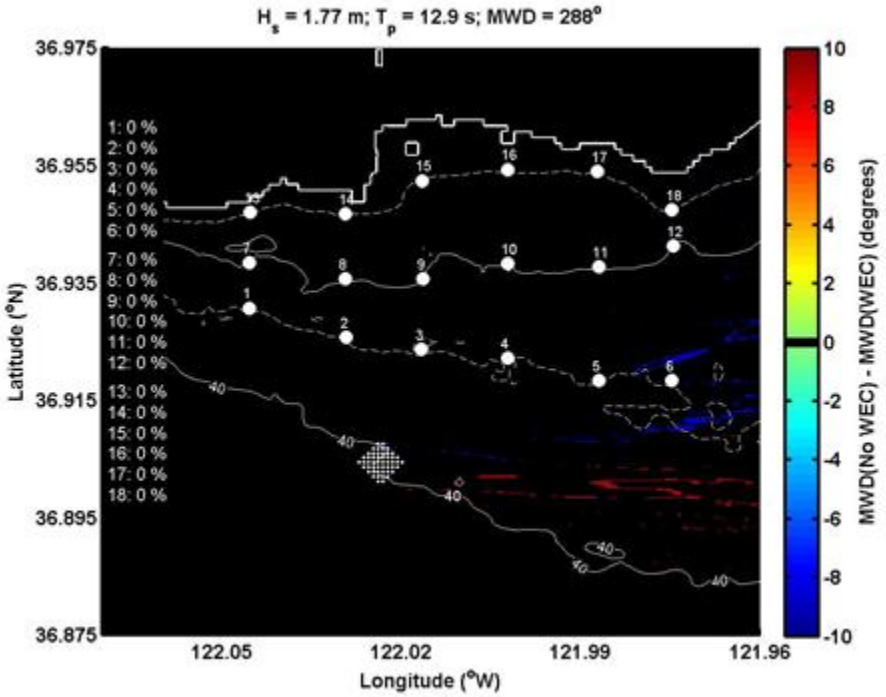

Figure 21. Same as caption for Figure 20 but for mean wave direction.

4.4.2 South Swell Conditions

Wave directions from <270° occurred 20% of the time and directions originating from <200° were observed 8% of the time in October 2009. The overall frequency of occurrence of wave directions was comparable to that of the 18 year wave record from the NOAA NDBC (Figure 3 and Figure 19). Because southerly waves impact the wave conditions along the Santa Cruz, CA shoreline, it was necessary to investigate these south swell conditions in greater detail.

Surface-to-surface comparison results for below average significant wave height (H_s = 1.15 m), above average wave period (T_p = 12.9 s), and mean wave direction directly from the south (MWD = 180°) are shown in Figure 22 and Figure 23. Wave height decreases of greater than 30% were found immediately downstream of the WEC array. These changes in wave heights decreased toward the shoreline, to values of about 10% at the 30 m and 20 m depth contour and near 5% at the 10 m depth contour. The largest wave height decreases were directly in the lee, to the north of the WEC array (output location numbers 3, 9, and 15; Figure 22). The along-shore extent of wave height reduction along the 10 m depth contour was limited to output location numbers 14 to the west and number 17 to the east.

Similarly, wave direction changes were minimal, with little along-shore (horizontal) extent. Maximum direction rotations were directly in the lee of the WECs. Clockwise rotation (negative changes) of wave directions were found slightly to the west of the center line of the WEC array and counter-clockwise rotation (positive changes) were found slightly to the east (Figure 23).

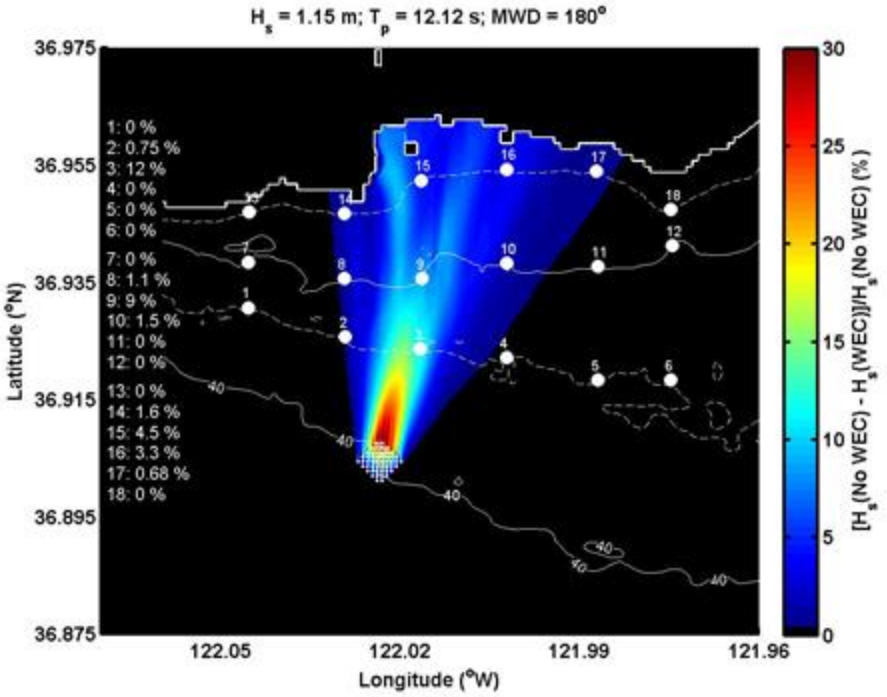

Figure 22. Significant wave height percentage decrease from the baseline scenario for South Swell wave conditions. Percent differences at each of the 18 output locations are indicated. Device diameters are not to scale.

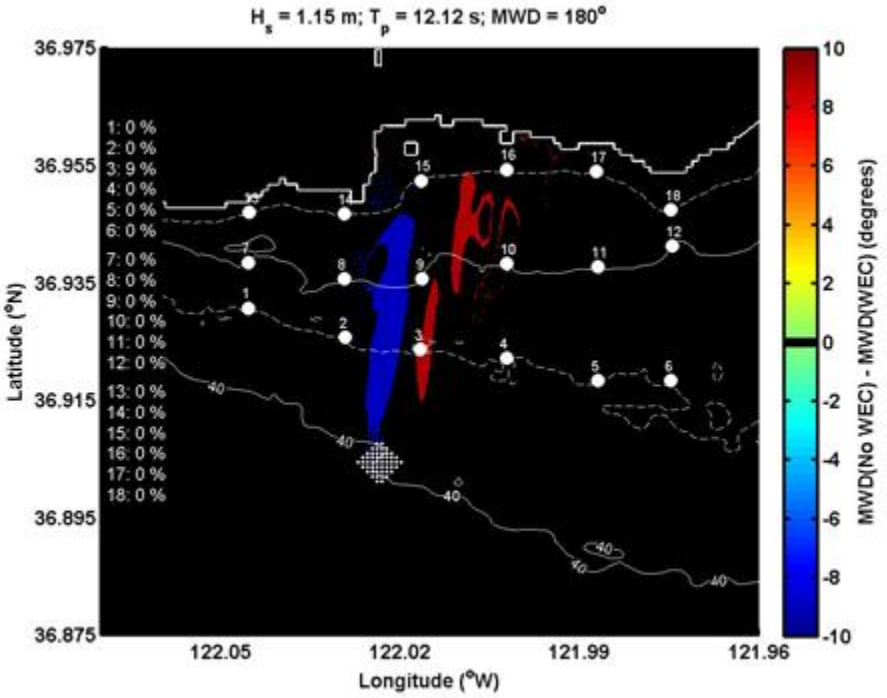

Figure 23. Same as the caption for Figure 22 but for mean wave direction.

4.4.3. Typhoon Conditions

The typhoon that affected the Monterey Bay, CA region was highly unusual, with wave directions of <180° and significant wave heights of >3.5 m. Over the 18 year NOAA NDBC wave record in Monterey Bay, CA, wave directions of 161° occurred less than 1% of the time and wave heights exceeding 3.5 m occurred about 5% of the time.

Results for the Typhoon conditions were similar to those for the South Swell case. However because of larger incident wave heights (H_s = 3.54 m), wave height reductions were near 40% directly in the lee of the WEC array (see power matrices in Figure 8). Decreases in wave height were more focused during the typhoon, with the highest wave height reduction found downstream of the WECs along the same angle as the incident wave direction, at output location number 14 (Figure 24). The along-shore spatial extent of wave height reduction was narrower than that observed during the South Swell conditions. Very little changes in wave direction were observed during the Typhoon over the domain; no change was observed at any of the output locations (Figure 25).

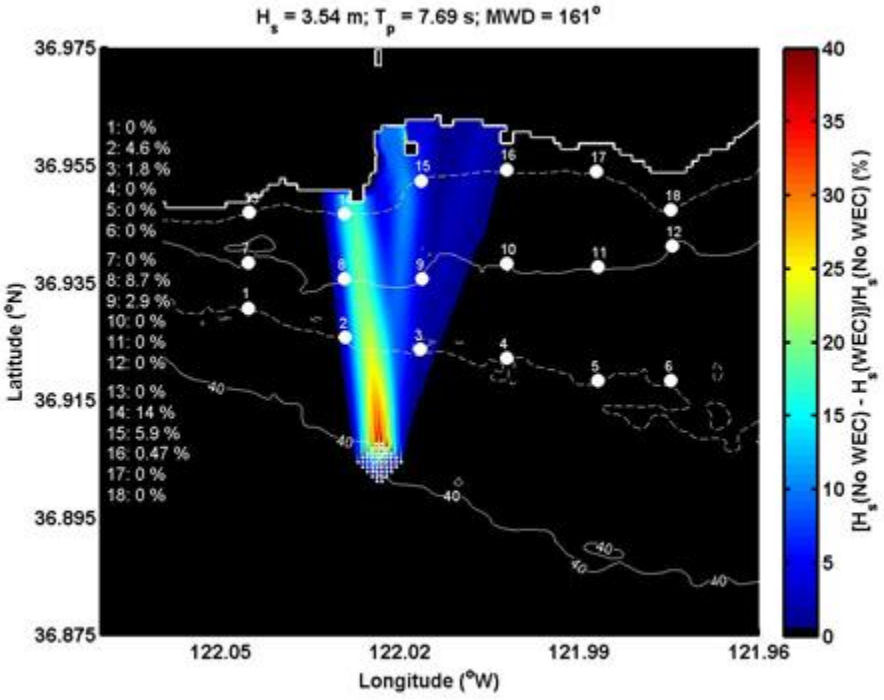

Figure 24. Significant wave height percentage decrease from the baseline scenario for Typhoon wave conditions. Percent differences at each of the 18 output locations are indicated on the left. Device diameters are not to scale.

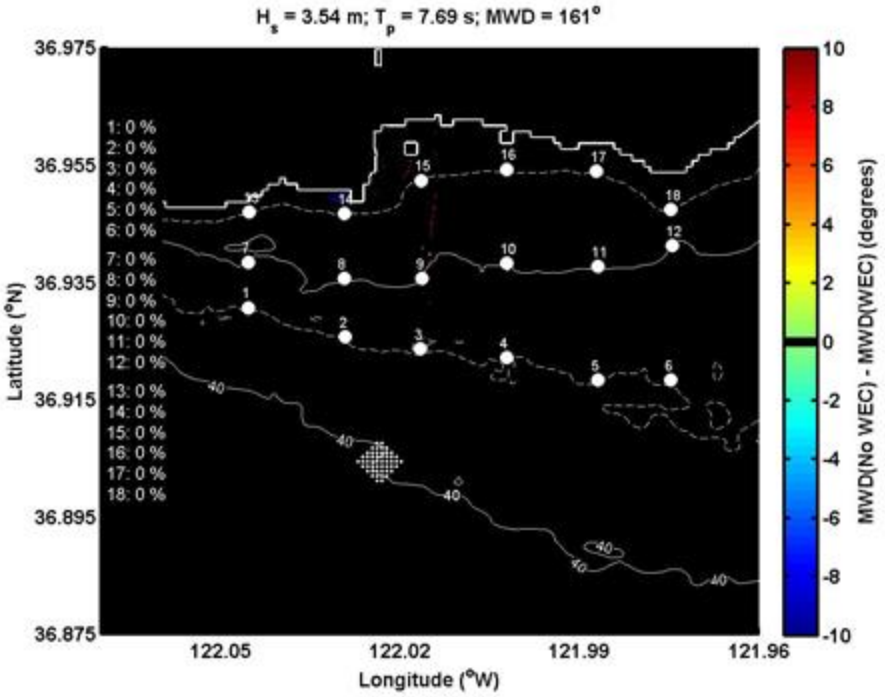

Figure 25. Same as the caption for Figure 24 but for mean wave direction.

4.5 Results Summary

SNL-SWAN model simulations were performed for hourly NOAA NDBC data obtained for the month of October 2009. The model was run with an array of 50 WECS of F-2HB or F-OWC device types centered on the 40 m depth contour. Results were compared with model runs without WECs and are summarized here.

- The percentage change in wave height between model runs with WECs and without WECs ranged from 0% to 15% in October 2009 for the 18 output locations in the Santa Cruz model domain.
- Maximum changes in H_s were found for locations downstream of the WEC array, along the angles of incident wave direction.
- Minimal changes in H_s were found for output locations along the western side of the Santa Cruz model domain due to wave shadowing by land.
- Output locations along the 30 m depth contour to the east of the WEC array exhibited >0.5% change in H_s at all times, including for initial wave directions of >270° due to their locations relative to the WEC array and wave refraction.
- The F-OWC device type resulted in greater reductions in wave heights in the lee of the WEC array due to its potential for capturing more power than the F-2HB device type.
- Changes in wave period were negligible, primarily due to model constraints.
- Mean wave direction variability due to the presence of WECs was limited to ±9° resolution and was observed at output locations only during southerly wave conditions.

- During average wave conditions observed in October 2009, the simulated WEC array had little effect on wave height or direction at the 18 output locations chosen for this modeling study.
- Waves originating from the south (~180°) resulted in >30% reductions in wave height directly in the lee of the WEC array. These reductions in H_s decreased toward the shoreline to percentage changes of ~5%.
- Extreme typhoon conditions observed in October 2009 resulted in 40% decreases in H_s in the lee of the WEC array and focused wave reductions along the Santa Cruz shoreline of up to 14%.

5. FUTURE WORK

The study presented here lays the groundwork for future analysis of seasonal effects of WEC arrays on nearshore wave dynamics. The SNL-SWAN model will be applied to real-world situations to assess the environmental effects created by changes in wave climates resulting from deployment of WEC farms in coastal waters. In order to achieve this, the following analyses will be conducted:

- Review the historical record of the Monterey Bay NDBC buoy data and assess general wave statistics and extreme events.
- Conduct SNL-SWAN model runs in the presence and absence of WEC arrays for average wave conditions for each season.
- Conduct SNL-SWAN model runs in the presence and absence of WEC arrays for extreme wave conditions that consider the upper 1% of wave statistics for each season.

The results from wave seasonality studies will be used to guide the selection of conditions with which to run full ocean circulation models that consider waves, currents, and winds. The ocean circulation model, coupled with sediment transport simulations, will indicate potential coastal geomorphological variability due to the presence of WEC arrays.

6. REFERENCES

1. Babarit, A., J. Hals, M.J. Muliawan, A. Kurniawan, T. Moan, and J. Krokstad, 2012, Numerical benchmarking study of a selection of wave energy converters, Renewable Energy, 41, 44-63.

2. Chang, G., J. Magalen, C. Jones, and J. Roberts, 2014, Wave Energy Converter Effects on Wave Fields: Evaluation of SNL-SWAN and Sensitivity Studies in Monterey Bay, CA, Tech. Rep. SAND2014-17460, Sandia National Laboratories, Albuquerque, NM, 77 pp.

DISTRIBUTION

4 Lawrence Livermore National Laboratory
Attn: N. Dunipace (1)
P.O. Box 808, MS L-795
Livermore, CA 94551-0808

1 MS0899 Technical Library 9536 (electronic copy)


Sandia National Laboratories